ADVANCED FUNCTIONAL MATERIALS
www.afm-journal.de

Superhydrophobic Carbon Nanotube Electrode Produces a Near-Symmetrical Alternating Current from Photosynthetic Protein-Based Photoelectrochemical Cells

Swee Ching Tan, Feng Yan, Lucy I. Crouch, John Robertson, Michael R. Jones, and Mark E. Welland*

The construction of protein-based photoelectrochemical cells that produce a variety of alternating currents in response to discontinuous illumination is reported. The photovoltaic component is a protein complex from the purple photosynthetic bacterium *Rhodobacter sphaeroides* which catalyses photochemical charge separation with a high quantum yield. Photoelectrochemical cells formed from this protein, a mobile redox mediator and a counter electrode formed from cobalt disilicide, titanium nitride, platinum, or multi-walled carbon nanotubes (MWCNT) generate a direct current during continuous illumination and an alternating current with different characteristics during discontinuous illumination. In particular, the use of superhydrophobic MWCNT as the back electrode results in a near symmetrical forward and reverse current upon light on and light off, respectively. The symmetry of the AC output of these cells is correlated with the wettability of the counter electrode. Potential applications of a hybrid biological/synthetic solar cell capable of generating an approximately symmetrical alternating current are discussed.

1. Introduction

At the heart of natural photosynthesis, reaction center pigment-proteins use harvested light energy to power a linear or cyclic flow of electrons.[1–3] Photochemical charge separation occurs in these systems with a quantum yield (event per photon absorbed) close to unity, and there is growing interest in how reaction center proteins can be directly exploited for device applications in photovoltaics, biosensing, photodetection, fuel synthesis and biocomputing.[4–15] Key to the development of these new hybrid technologies is the effective interfacing of proteinaceous reaction centers with man-made materials.

A fundamental feature of solar cells based on doped silicon, photoactive dyes or polymer blends[16] is that illumination produces a flow of direct current (DC) that rapidly drops to zero if illumination is terminated. Photoelectrochemical cells based on electrodes coated with a variety of photosynthetic proteins have been observed to produce a similar light-dependent DC output.[17–25] However, novel protein-based photoelectrochemical cells have recently been described that produce a conventional DC in response to continuous illumination, but an unusual alternating current (AC) under conditions of discontinuous illumination.[26] These cells use as the photovoltaic material either the reaction center pigment-protein from the purple bacterium *Rhodobacter* (*Rba.*) *sphaeroides*, or the so-called RC-LH1 complex that is formed between this reaction center and an encircling LH1 light harvesting protein.[27] As shown in **Figure 1**a, in both types of protein the absorption of light energy produces a high quantum yield photochemical charge separation in which a pair of bacteriochlorophyll molecules at one end of the reaction center protein (denoted P) is oxidized and a ubiquinone at the other end of the protein (denoted Q_B) is reduced. Photoelectrochemical cells were fabricated by encapsulating solutions of reaction centres or RC-LH1 complexes and the redox mediator *N,N,N′,N′*-tetramethyl-*p*-phenylenediamine (TMPD) in a ≈10 µL volume cavity between a transparent FTO-glass front electrode and a back electrode formed from platinum-coated FTO-glass. Illumination of these cells produced a steady DC, but when illumination was switched off the current output did not drop to zero in the conventional manner but rather flowed in the reverse direction for approximately 20s. Modulation of illumination at a suitable frequency therefore elicited an AC output that was stable over multiple light-on/light-off cycles.[26]

Dr. S. C. Tan,[+] Prof. M. E. Welland
Nanoscience Centre
University of Cambridge
11 JJ Thomson Avenue, Cambridge CB3 0FF, UK
E-mail: sctan@mit.edu
Dr. F. Yan, Prof. J. Robertson
Engineering Department
University of Cambridge
9 JJ Thomson Avenue, Cambridge, CB3 0FA, UK
Dr. L. I. Crouch,[++] Dr. M. R. Jones
School of Biochemistry
University of Bristol
University Walk, Bristol BS8 1TD, UK
[+]Present address: Department of Materials Science and Engineering, Massachusetts Institute of Technology, 77 Massachusetts Avenue, Cambridge, MA 02139, USA
[++]Present address: Institute for Cell and Molecular Biosciences, Medical School, University of Newcastle, Newcastle upon Tyne, NE2 4HH, UK

DOI: 10.1002/adfm.201301057

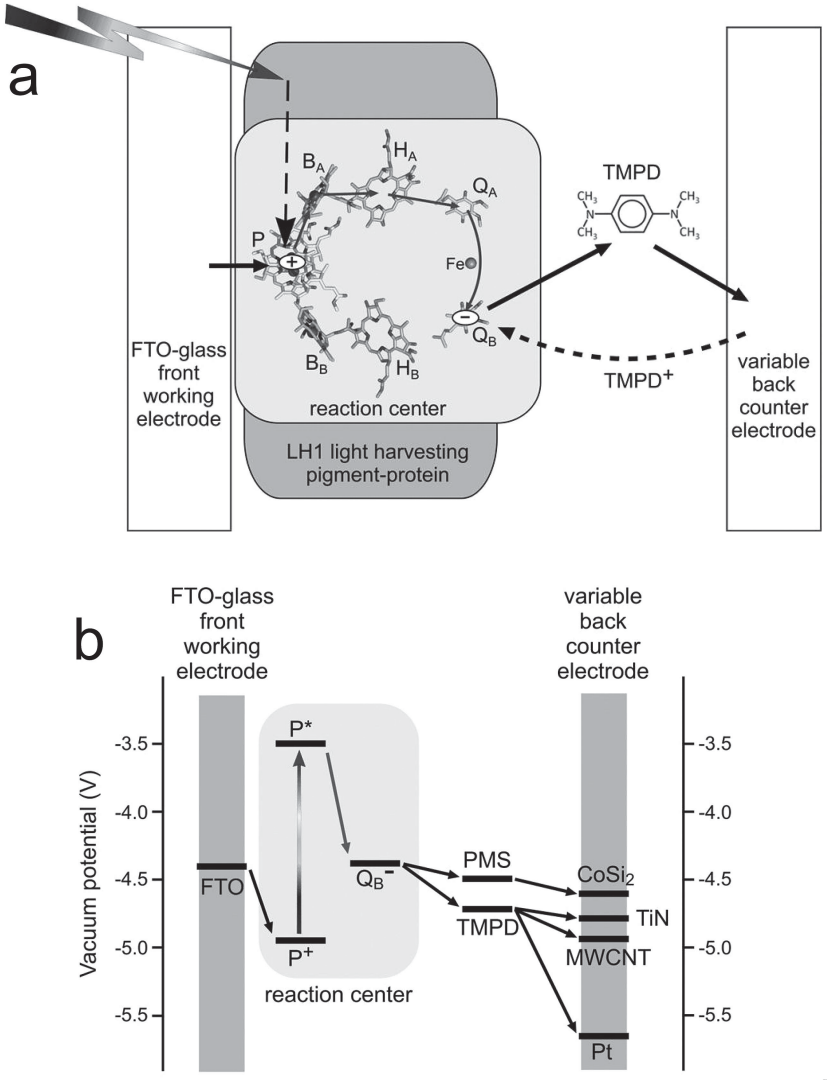

Figure 1. Composition and mechanism of protein photoelectrochemical cells. a) Schematic of light-powered electron transfer by RC-LH1 complexes that are closely associated with the FTO-glass front electrode. Photons are absorbed mainly by the bacteriochlorophyll and carotenoid pigments of the LH1 light harvesting pigment-protein, and excitation energy is passed by Förster transfer (dashed arrow) to a pair of "primary electron donor" bacteriochlorophylls (P) in the central reaction center protein. Photo-excitation of P triggers a charge separation through the cofactors of the reaction centre (thin grey arrows) to form a primary donor cation (P^+) at one end of the reaction centre protein and a reduced quinone (Q_B^-) at the other. P^+ is reduced by the adjacent FTO-glass electrode whilst electrons are shuttled from Q_B to the back electrode by the TMPD electrolyte (solid black arrows). b) Schematic showing the vacuum potentials of key components. Photoexcitation of P to P* changes its redox potential and triggers electron transfer to the Q_B quinone. With TMPD or, for $CoSi_2$, PMS as mediator a flow of direct current is observed to the back electrode.

Mechanisms accounting for the DC and AC outputs of cells of this design have been formulated on the basis of the direction of current, the vacuum potentials of the components of the cell (Figure 1b), known electron transfer properties of the mediator and the multiple redox cofactors of the reaction center, the relative hydrophilicities of the electrode materials, action spectra of current density and the effects of a reaction center inhibitor,[26] together with the results of varying the electrolyte solution to boost the open circuit voltage (V_{OC}).[28] A characteristic excitation wavelength dependence of the DC density, and the absence of a DC output in the presence of an inhibitor of electron transfer through the reaction center protein, demonstrated that the source of the DC was photochemical charge separation between the bacteriochlorophyll and quinone cofactors of the reaction center protein, shown schematically in Figure 1a. As only a single redox mediator was employed it was reasoned that the photoactive RC-LH1 complexes adhere to one of the cell's two electrodes, facilitating a direct electrical contact between this working electrode and one of the two possible "terminals" of the RC-LH1 complex, with the TMPD mediator shuttling electrons from the other terminal of the RC-LH1 protein to the counter electrode.[26] It was concluded that it was more likely that the FTO-glass front electrode would bind the photoactive protein (Figure 1a), as this material is much more hydrophilic than the Pt used for the back electrode (as inferred from measured contact angles with a 5 μL droplet of water of 18.7° and 93.8°, respectively[26]). In the derived mechanism for the DC output from this cell (Figure 1a), photochemical charge separation produced electrons at the quinone terminal of the reaction center protein (Q_B^-) that were shuttled to the counter electrode by the TMPD mediator (Figure 1a), with the photo-oxidized terminal of the reaction centre protein (P^+) being re-reduced by electrons from the adjacent FTO-glass anode (Figure 1a). This mechanism is consistent with the vacuum potentials for TMPD, the two electrodes and the P^+ and Q_B^- redox centers within the reaction center protein (Figure 1b).[26]

Regarding the mechanism underlying the AC output under discontinuous illumination, a reproducible feature of the short circuit current (J_{SC}) recorded immediately after the onset of illumination was a ≈10–20 s transient spike that was attributed to an over-reduction of the multiple electron transfer cofactors within each reaction center, and an accompanying over-oxidation of the TMPD/$TMPD^+$ electrolyte solution. A representative current profile for a cell formed from RC-LH1 protein with Pt as the counter electrode is shown in **Figure 2**a. Creation of this difference in potential between the reaction center and TMPD 'compartments' was consistent with documented slow oxidation of the reaction center quinone cofactors by $TMPD^+$ creating a bottleneck for electron flow within the cell.[26] Under continuous illumination a conventional steady DC was produced in the period after the initial spike of current flow had decayed, indicated by the dashed line in Figure 2a.

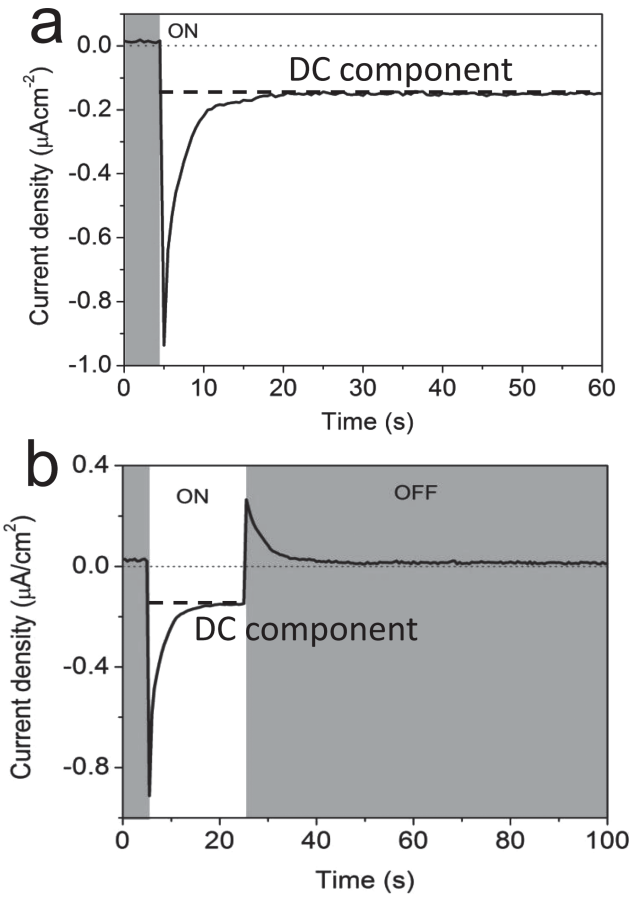

Figure 2. Characteristics of DC and AC output of Pt/TMPD photoelectrochemical cells. a) Time dependence of J_{SC} produced under continuous illumination. b) Time dependence of J_{SC} produced in response to a single 20 s period of illumination. The amplitude of the DC component during illumination is indicated by the dashed line.

However, on switching off illumination to such a cell an unusual transient reverse current was observed (positive deflection at $t = 26$ s in Figure 2b) that represented discharge of the potential difference between the over-reduced reaction center cofactors and the over-oxidized TMPD/TMPD$^+$ electrolyte through the external circuit connecting the electrodes of the cell.[26] This alternating forward/reverse output was seen reproducibly in response to multiple light-on/light-off cycles, and was obtained even if electron transfer through the reaction centre quinone sites was blocked using an inhibitor thus preventing photogeneration of DC.[26] The actual kinetics of the spikes of forward and reverse current following light-on and light-off events may have been influenced by diffusion of the electrolyte in response to the developments and dissipation, respectively, of the potential difference within the cell.

As well as providing a source of direct photocurrent for applications in photovoltaics, photocatalysis and biosensing, cells of this type also therefore produce an alternating photocurrent that has the potential to be exploited in novel ways (see below). However, a possible drawback in the further development of this hybrid technology towards device applications is the use of platinum, a rare and extremely expensive metal, as the back electrode. The present work therefore set out to explore the ability of an electrode formed from multi-walled carbon nanotubes (MWCNTs) to support both direct and alternating currents from protein-based photoelectrochemical cells. During the course of this it was discovered that the material used for the counter electrode has a strong influence on the symmetry of the AC obtained under discontinuous illumination, the likely origin being the propensity of this material to interact with the proteins that support the flow of photocurrent. This finding opens up the prospect of being able to fabricate cells capable of different types of DC and/or AC output by exploiting different combinations of photoactive proteins, mediators and man-made materials.

2. Results and Discussion

To provide an alternative counter electrode for the fabrication of a protein-based photoelectrochemical cell, "forests" of MWCNTs were grown on a cobalt disilicide substrate according to a procedure described recently.[29] Cobalt disilicide was selected as the substrate because it has resistivity as low as Au and Pt and is commonly used as contacts in CMOS devices.[30,31] Tunneling electron microscopy (TEM) showed that a typical MWCNT had a diameter of around 15 nm and was made up from ten layers of graphene sheet (**Figure 3**a). The layer of MWCNTs exhibited the expected superhydrophobicity,[32,33] a 5 μL drop of deionised water placed on the MWCNT substrate displaying a very high contact angle of 160.9° (Figure 3b). The morphology of the resulting MWCNT forest was examined by scanning electron microscopy (SEM), revealing a closely packed and entangled layer with a height of approximately 7 μm (Figure 3c). These characteristics were retained following prolonged immersion of the MWCNT layer in liquid, its morphology being essentially unaffected by submersion under a ≈1 cm layer of deionised

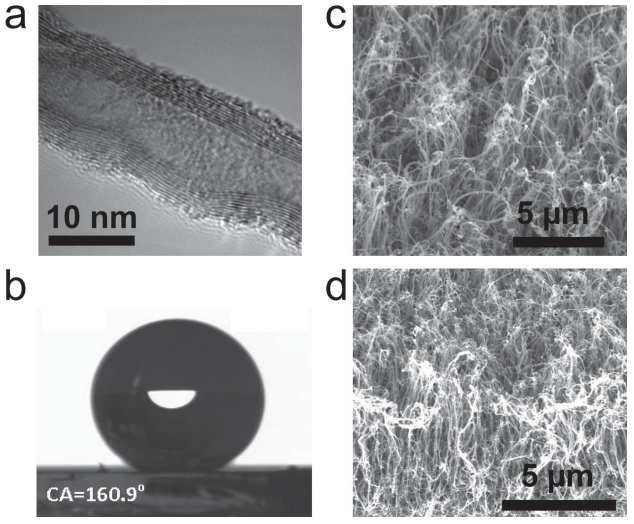

Figure 3. a) Tunneling electron microscopy image of a single CNT. b) CCD camera image of a ≈5 μL drop of deionised water placed on a MWCNT surface; contact angle = 160.9°. Scanning electron microscopy images c) at 45° to a MWCNT surface before wetting, and d) at 45° to a MWCNT surface after wetting and drying in air.

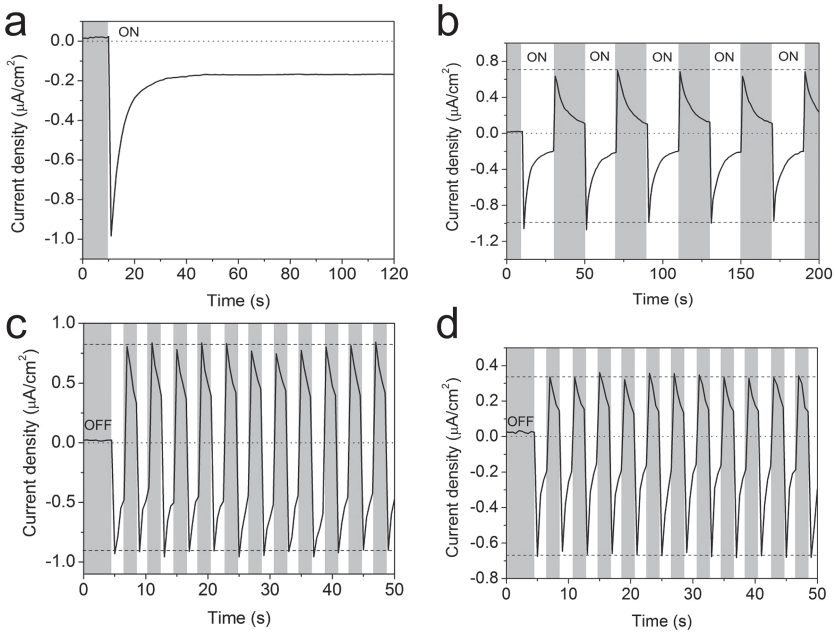

Figure 4. Time dependence of J_{SC} produced by a) a MWCNT/TMPD cell under continuous illumination, b) a MWCNT/TMPD cell exposed to 20 s light-on/light-off cycles, c) a MWCNT/TMPD cell exposed to 2 s light-on/light-off cycles, d) a Pt/TMPD cell exposed to 2 s light-on/light-off cycles.

water for 24 h, followed by drying in air (Figure 3c, compared with Figure 3d).

Photoelectrochemical cells employing MWCNTs as the back electrode were fabricated using the simple procedure described in the Experimental Section, with a mixture of purified RC-LH1 protein and TMPD electrolyte solution being injected into a narrow cavity between a fluorine-doped tin oxide (FTO) glass front electrode and the MWCNT back electrode. Photochronoamperometry of such MWCNT/TMPD cells was conducted under conditions of either continuous or modulated illumination from white light passed through a 570 nm long-pass filter. Illumination of a MWCNT/TMPD cell produced a spike of current flow immediately upon illumination that settled down over a period of ≈40 s to a steady J_{SC} of ≈170 nA/cm^2 (**Figure 4**a), similar in magnitude and direction to the ≈150 nA/cm^2 current seen previously for RC-LH1 cells with a Pt-coated back electrode (Figure 2a).[26] The direction of current flow was from the FTO-glass front electrode into the device, and for convenience this is henceforth referred to as "forward current". Exposure to discontinuous illumination (alternating 20 s periods of light and dark) resulted in spikes of rapid forward current following each dark-to-light transition, and a similar reverse current following each light-to-dark transition (Figure 4b). This cell therefore displayed the AC seen previously for equivalent Pt/TMPD cells, but notably the maximum amplitude of the reverse current was up to three times larger than seen previously in equivalent Pt/TMPD cells.[26] This difference in the relative amplitudes of the forward and reverse currents was seen in multiple devices. Figures 4c,d compare the AC output of MWCNT/TMPD and Pt/TMPD cells exposed to 2 s light-on/light-off cycles; the initial amplitude of the reverse current was ≈90% that of the forward current in the former compared to <50% in the latter.

Given that the other components were unchanged, this increased symmetry of the AC output must have been attributable to the change in the material used for the back electrode from Pt to MWCNTs. A notable difference between the two materials is their wettability, a property that could be of significance if the output of cells of this type has the potential to be modulated to some extent by unproductive adherence of protein to the back electrode. It would be expected that the extent of protein adherence should be affected by wettability, and should be minimal for a superhydrophobic material such as a MWCNT forest (**Figure 5**a) but greater for a less hydrophobic material such as Pt (Figure 5b). Where it occurs to a significant extent such protein adherence could physically block access of the electrolyte to the back electrode. In addition, as illustrated by the white arrows in Figure 5b, it is also possible that the current output characteristics of the device immediately after termination of illumination could be modulated through electron tunneling between the back electrode and adhered, photo-activatable protein. Some indication of the latter was seen on comparing the V_{OC} produced by Pt/TMPD and MWCNT/TMPD cells under continuous illumination, a parameter that has recently been shown to be linearly dependent on the vacuum potential of the electrolyte that shuttles electrons to the back electrode.[28] The measured V_{OC} was higher for the MWCNT cell than for the otherwise identical Pt cell (Figure S1a of the Supporting Information), which could be taken as evidence that the V_{OC} of the Pt/TMPD cell was attenuated by interactions between the Pt electrode and a layer of adhered protein. A similar finding was obtained with Pt and MWCNT cells fabricated with a more reducing mediator, phenazine methosulphate (PMS), as the electrolyte (Figure S1b of the Supporting Information); the cells with a superhydrophobic MWCNT counter electrode produced a much higher steady V_{OC}.

The dependence of the symmetry of the AC output on the wettability of the counter electrode was examined further using alternative materials. Fabrication of the MWCNT electrode involved the preparation of a $CoSi_2$ surface to act as a base layer, and as part of that process a 20 nm thick TiN film was used as a capping layer to prevent oxidation of Co during silicidation.[34] Both of these materials can act as electrodes,[35] and have work functions in the same region as MWCNTs (−4.62 eV for $CoSi_2$[36,37] and −4.8 eV for TiN[38] compared to −4.95 eV for MWCNTs[39] (Figure 1b)). However both $CoSi_2$ and TiN are markedly more hydrophilic than MWCNTs, yielding contact angles with a droplet of water of 53.2° and 64.3°, respectively (Figure S2; Supporting Information), intermediate between previously measured values for a Pt electrode (93.8°)[26] and for the highly hydrophilic FTO-glass front electrode (18.7°).[26] Following the argument presented above, the expectation was therefore that both $CoSi_2$ and TiN would be more prone to binding RC-LH1 protein than Pt (Figure 5b compared with

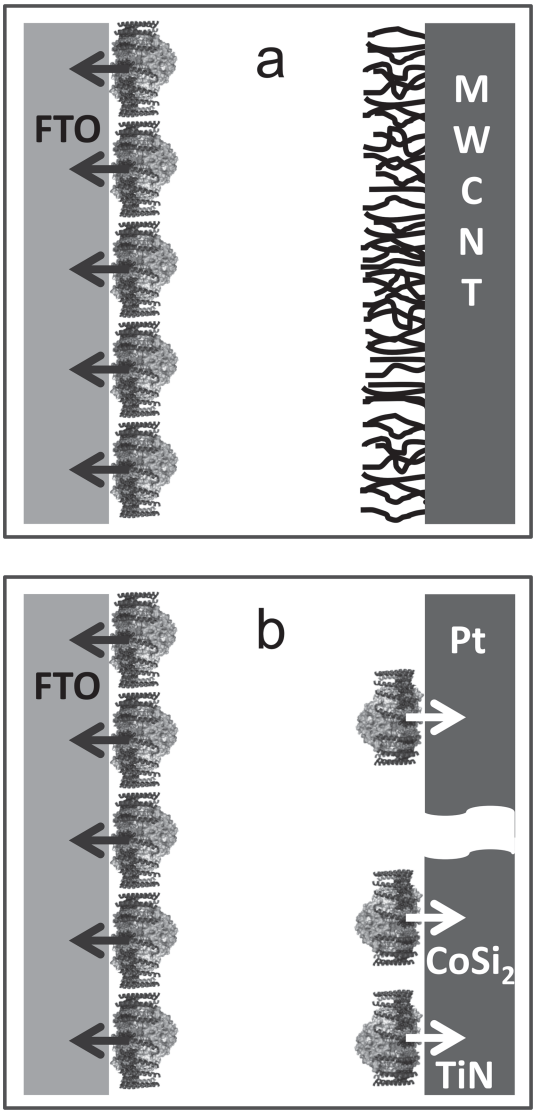

Figure 5. Schematics of protein adherence in photoelectrochemical cells with a) MWCNT or b) Pt or TiN/$CoSi_2$ counter electrodes. Arrows show possible electron donation to electrodes following cessation of illumination that contribute to (dark grey) or attenuate (white) the extent of reverse current flow.

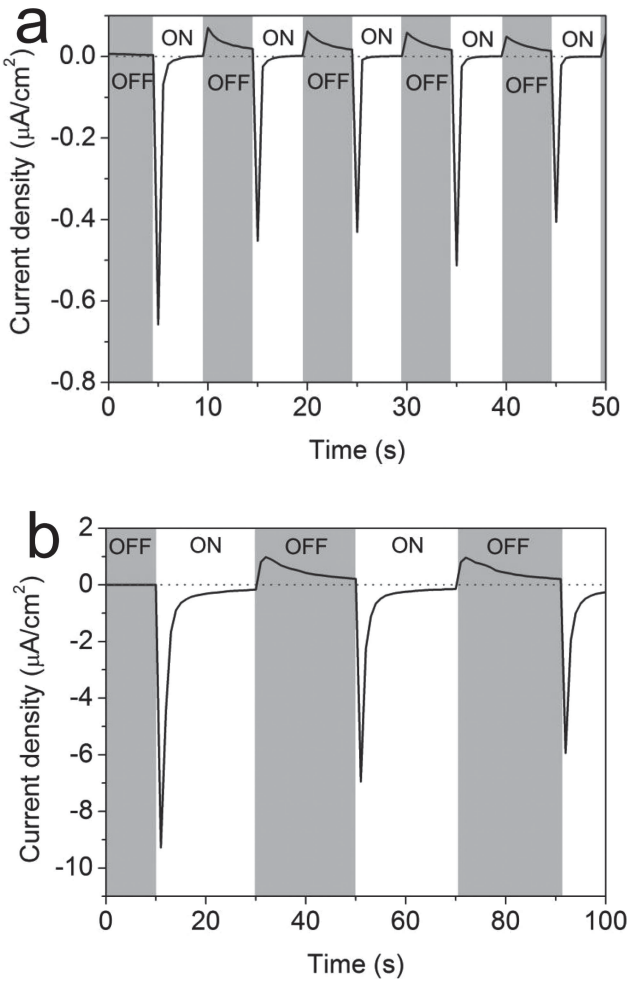

Figure 6. Time dependence of J_{SC} produced by a) a $CoSi_2$/TMPD cell exposed to 5 s light-on/light-off cycles or b) a TiN/TMPD cell exposed to 20 s light-on/light-off cycles.

Figure 5a), with the prediction that these materials should support a less symmetrical AC output than Pt.

Cells assembled using a $CoSi_2$ electrode and filled with a mixture of RC-LH1 protein and TMPD produced a light-induced spike of current flow that dropped to zero within a couple of seconds (**Figure 6**a), with no subsequent steady-state DC (see Supporting Information Figure S3a for a single light-on/light-off cycle). The reason for this is discussed below. However, an AC was obtained from $CoSi_2$/TMPD cells (Figure 6a), exposure to alternating 5 s periods of light and dark resulting in spikes of rapid forward current following each dark-to-light transition, and a lower amplitude and more slowly decaying reverse current following each light-to-dark transition. Cells assembled using a TiN electrode were able to support both an AC and a DC, the latter having an amplitude of ≈140 nA/cm^2 after a relatively large spike of initial photocurrent flow (Figure 6b; and see a trace recorded under continuous illumination in Supporting Information Figure S3c). In the case of the AC it was striking that the peak amplitude of the forward current, typically ≈7000 nA/cm^2 was much larger than the 500–1000 nA/cm^2 observed for Pt, $CoSi_2$ or MWCNT-based cells, and the peak reverse current was also proportionately larger. Irrespective of absolute amplitude however, both the TiN and $CoSi_2$ cells produced a markedly less symmetrical AC than that observed for either the MWCNT or Pt cells (Figure 6a,b compared with Figure 4c,d), with in both cases the peak amplitude of the forward current being several times larger than that of the reverse current.

A likely explanation for the absence of a DC output from the $CoSi_2$/TMPD cells was that the work function of $CoSi_2$ (–4.62 eV)[36,37] is too reducing for it to act as an electron acceptor from the TMPD mediator (at –4.73 eV)[40] (Figure 1b). To investigate this, cells with a $CoSi_2$ back electrode were also fabricated with PMS as electrolyte, as this has a vacuum potential of –4.51 eV[40] which is more reducing than that of either

Table 1. Characteristics of AC output from protein cells with different back electrodes.

Back electrode	AC forward maximum[a)] [nA/cm^2]	AC reverse maximum[a)] [nA/cm^2]	AC symmetry[b)]	Electrode Contact Angle [°]	Resistivity [μΩ cm]
MWCNT	1000	800	0.800	160.9	10[41]
Pt	≈900	300	0.333	93.8	10[42]
TiN	7000	1000	0.142	64.3	10[43]
$CoSi_2$	500	50	0.100	53.2	40[30]

[a)]Typical values from multiple light-on/light-off cycles; [b)]Maximum reverse current divided by maximum forward current.

TMPD or $CoSi_2$ (Figure 1b). Under continuous illumination these $CoSi_2$/PMS cells produced an initial spike of forward current followed by modest steady DC of ≈10–15 nA/cm^2 (Supporting Information Figure S3b), supporting the conclusion that a steady photo-induced DC output from cells of this design was dependent on the relative vacuum potentials of the electrolyte and the back electrode.

Summarizing the data obtained under discontinuous illumination, an AC output was obtained from photoelectrochemical cells containing RC-LH1 protein and TMPD irrespective of whether the back electrode was fabricated from Pt, $CoSi_2$, TiN or MWCNTs, but the symmetry of the AC varied considerably. Typical maximum amplitudes for the forward and reverse components of the AC obtained from the various cells are collated in **Table 1**, as are the measurements of contact angle for the back electrode specified above, and a measure of the symmetry of the AC obtained by expressing the typical peak reverse current as a function of the typical peak forward current. As can be seen from the plot of the latter two parameters in **Figure 7**, the symmetry of the AC signal increased approximately linearly with increasing hydrophobicity of the back electrode. Although the reason for this trend remains to be proven, as argued above a likely source is a decreased propensity for protein to adhere to the back electrode as its wettability decreases. Table 1 also details the resistivity of the electrode material;[30,41–43] there was no correlation between this parameter and the symmetry of the AC signal.

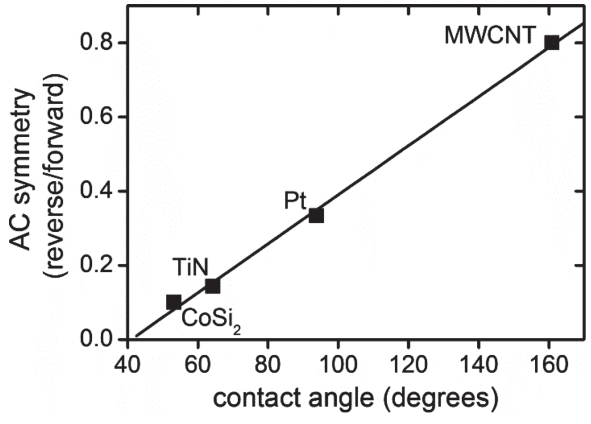

Figure 7. Correlation between the symmetry of the AC output of the protein photoelectrochemical cells and the wettability of the counter electrode.

Turning to the underlying motivations for this work, photoelectrochemical cells incorporating photosynthetic proteins have a number of potential applications, perhaps the most discussed being as biosensors for herbicides such as atrazine that block electron flow through the Q_B quinone binding site of the purple bacterial reaction center and its higher plant counterpart Photosystem II.[6–9] The unusual AC capacity of the cells described above represents an additional property that can be exploited for applications, particularly if the forward and reverse current components were to be made fully symmetrical. The most obvious is as a direct source of light-generated AC, something that solar cells cannot normally achieve because their design limits them to producing a DC that has to be processed through an inverter. In addition, as outlined in Supporting Information (Figure S4), two such cells wired in tandem could be used to construct a macroscale optical XNOR logic gate, the inputs being the switching of excitation light from off to on or on to off, and the output being the sum of the currents from the two cells. Although these properties are described in the context of two macroscopic protein cells, each containing a population of photoproteins, the same characteristics would apply to much smaller ensembles of RC-LH1 molecules adhered to a conducting surface. It is worth noting that two of the major challenges in the development of nanoscale molecular logic gates are the integration of such devices with conventional electronic components, and the transition from ensembles to individual molecules. It is now well established that photoreaction centres can be interfaced with conducting metal surfaces in a productive manner,[17–25] and these proteins are also at the forefront of research on nanoscale patterning of molecules on surfaces (e.g. see ref. [44]), and the spectroscopic[45] or electrical[46,47] analysis of single molecules.

3. Conclusions

Four photoelectrochemical cells were fabricated with a photosynthetic protein as the photovoltaic component, transparent FTO-glass as the front electrode and a variety of materials as the back electrode. A DC output was obtained from all four cells provided that a redox mediator was used with a vacuum potential intermediate between that of the quinone redox centre of the protein and the back electrode. An AC output was obtained during discontinuous illumination of photoelectrochemical cells containing TMPD as the redox mediator irrespective of whether the back electrode was fabricated from Pt, $CoSi_2$, TiN, or MWCNTs. However the symmetry of the AC varied considerably between the cells, in a manner which correlated with the wettability of the material used for the back electrode. The likely source of this variation is a decreased propensity for protein to adhere to the back electrode as its wettability decreases, the use of a superhydrophobic layer of MWCNTs as the back electrode producing a near symmetrical AC. The results demonstrate that the current output of protein-based photoelectrochemical cells can be tailored to specific requirements through manipulation of illumination conditions, the materials used for the electrodes and the mediator used for transfer of electrons within the cell.

4. Experimental Section

Growth of MWCNTs: MWCNTs were grown on $CoSi_2$ substrates using a cold wall chemical vapor deposition (CVD) system.[32] $CoSi_2$ substrates were evaporated with 1 nm of Fe which acted as a catalyst for the growth of MWCNTs. The Fe/$CoSi_2$/Si substrates were then loaded into a cold wall CVD chamber and heated to 580 °C in 200 sccm of H_2 for 5 mins to reduce any FeO_x to Fe. The heating caused the film to crack and break into nano-sized catalyst clusters. To grow MWCNT, C_2H_2 and H_2 in the ratio of 5 sccm:195 sccm were introduced into the chamber during a 5 min growth process and the substrates were maintained at 580 °C. The C_2H_2 decomposed to form carbon atoms which were then precipitated on the nano-sized Fe catalyst to form CNTs. 200 sccm of H_2 was introduced into the chamber to flush out unreacted C_2H_2, the heater was turned off and the chamber allowed to cool to room temperature.

Characterization of MWCNTs: The morphology of the MWCNT layer was characterized by high resolution SEM using a FEI XL30 FEG-SEM. Cross-sectional images of individual MWCNTs were characterized by a Phillips CM300 TEM. Five MWCNTs were characterized and all had a diameter of ≈14 nm ± 3 nm. Contact angle measurements were carried out using a KSV CAM 200 goniometer. Four MWCNT films were measured and the contact angle was found to be highly reproducible (161.5° ± 1.8°).

Fabrication of Photoelectrochemical Cells: RC-LH1 complexes from *Rba. sphaeroides* were purified as described in detail previously.[26] To fabricate the cells, FTO conducting glass (TEC 15 ohm/sq, 20 mm square × 2.2 mm thick (Solaronix, Switzerland) was used as the transparent front electrode and the $CoSi_2$ substrate with a MWCNT film as the back electrode. Alternatively a bare $CoSi_2$ substrate, or a $CoSi_2$ overlaid by a 20 nm layer of TiN was used as the back electrode. Before use the FTO-glass substrates were cleaned by sonication with acetone followed by isopropanol. A U-shaped piece of hot-melt sealing foil of 75 μm thickness (Dupont) was used to join the two electrodes, creating a cavity with an opening at one side. A 10 μL aliquot of a mixture of RC-LH1 or reaction center complexes and TMPD at final concentrations 85 μM and 250 μM, respectively was injected into this cavity, the mixture flowing into the cavity by capillary action. Once the cell was filled the opening was sealed with a rapid setting-epoxy (Araldite).

Electrical measurements: Photochronoamperometry was performed using illumination from a 100 W incandescent lamp passed through a 570-nm-long pass filter, such that the incident light intensity at the surface of the cell was a constant 10 mW/cm^2. Discontinuous illumination was achieved through use of a shutter. To account for variations in the active area of individual cells a black mask with an aperture of 0.21 cm^2 was placed in front of the FTO-glass electrode before measurement to standardize the area illuminated. Photocurrents were recorded under short circuit conditions using a 2636A SourceMeter (Keithley).

Supporting Information

Supporting Information is available from the Wiley Online Library or from the author.

Acknowledgements

SCT acknowledges scholarships from Cambridge Commonwealth Trust and Wingate Foundation. LIC and MRJ acknowledge funding from the Biotechnology and Biological Sciences Research Council of the United Kingdom. We would like to thank Dr C. Zhang for the assistance in TEM imaging of the MWCNT.

Received: March 27, 2013
Revised: May 7, 2013
Published online: June 14, 2013

[1] J. Deisenhofer, H. Michel, *Science* **1989**, *245*, 1463.
[2] P. Heathcote, P. K. Fyfe, M. R. Jones, *Trends Biochem. Sci.* **2002**, *27*, 7.
[3] P. Heathcote, M. R. Jones, in *Comprehensive Biophysics* Vol. *8* (Eds: E. H. Egelman, S. Ferguson), Academic Press, Oxford, UK **2012**, p. 115.
[4] D. A. LaVan, J. N. Cha, *Proc. Natl. Acad. Sci. USA* **2006**, *103*, 5251.
[5] Y. Lu, J. Xu, B. Liu, J. Kong, *Biosens. Bioelectron.* **2007**, *22*, 1173.
[6] M. T. Giardi, V. Scognamiglio, G. Rea, G. Rodio, A. Antonacci, M. Lambreva, G. Pezzotti, U. Johanningmeier, *Biosens. Bioelectron.* **2009**, *25*, 294.
[7] C. A. Sanders, M. Rodriguez, E. Greenbaum, *Biosens. Bioelectron.* **2001**, *16*, 439.
[8] V. Scognamiglio, G. Pezzotti, I. Pezzotti, J. Cano, K. Buonasera, D. Giannini, M. T. Giardi, *Microchim. Acta* **2010**, *170*, 215.
[9] A. Ventrella, L. Catucci, A. Agostiano, *Bioelectrochem.* **2010**, *79*, 43.
[10] G. LeBlanc, G. Chen, E. A. Gizzie, G. K. Jennings, D. E. Cliffel, *Adv. Mater.* **2012**, *24*, 5959.
[11] H. Nishihara, K. Kanaizuka, Y. Nishimori, Y. Yamanoi, *Coordin. Chem. Rev.* **2007**, *251*, 2674.
[12] L. Frolov, Y. Rosenwaks, S. Richter, C. Carmeli, I. Carmeli, *J. Phys. Chem. C* **2008**, *112*, 13426.
[13] M. Kato, T. Cardona, A. W. Rutherford, E. Reisner, *J. Am. Chem. Soc.* **2012**, *134*, 8332.
[14] H. Krassen, A. Schwarze, B. Friedrich, K. Ataka, O. Lenz, J. Heberle, *ACS Nano* **2009**, *3*, 4055.
[15] N. Terasaki, N. Yamamoto, K. Tamada, M. Hattori, T. Hiraga, A. Tohri, I. Sato, M. Iwai, M. Iwai, S. Taguchi, I. Enami, Y. Inoue, Y. Yamanoi, T. Yonezawa, K. Mizuno, M. Murata, H. Nishihara, S. Yoneyama, M. Minakata, T. Ohmori, M. Sakai, M. Fujii, *Biochim. Biophys. Acta* **2007**, *1767*, 653.
[16] M. Grätzel, *Nature* **2001**, *414*, 338.
[17] S. A. Trammell, A. Spano, R. Price, N. Lebedev, *Biosens. Bioelectron.* **2006**, *21*, 1023.
[18] J. Xu, Y. Lu, B. Liu, C. Xu, J. Kong, *J. Solid State Electrochem.* **2007**, *11*, 1689.
[19] M. Ciobanu, H. A. Kincaid, V. Lo, A. D. Dukes, G. K. Jennings, D. E. Cliffel, *J. Electroanal. Chem.* **2007**, *599*, 72.
[20] C. J. Faulkner, S. Lees, P. N. Ciesielski, D. E. Cliffel, G. K. Jennings, *Langmuir* **2008**, *24*, 8409.
[21] M. H. Ham, J. H. Choi, A. A. Boghossian, E. S. Jeng, R. A. Graff, D. A. Heller, A. C. Chang, A. Mattis, T. H. Bayburt, Y. V. Grinkova, A. S. Zeiger, K. J. Van Vliet, E. K. Hobbie, S. G. Sligar, C. A. Wraight, M. S. Strano, *Nat. Chem.* **2010**, *2*, 929.
[22] H. Yaghoubi, Z. Li, D. Jun, R. Saer, J. E. Slota, M. Beerbom, R. Schiaf, J. D. Madden, J. T. Beatty, A. Takshi, *J. Phys. Chem. C* **2012**, *116*, 24868.
[23] M.-J. den Hollander, J. G. Magis, P. Fuchsenberger, T. J. Aartsma, M. R. Jones, R. N. Frese, *Langmuir* **2011**, *27*, 10282.
[24] E. P. Lukashev, V. A. Nadtochenko, E. P. Permenova, O. M. Sarkisov, A. B. Rubin, *Doklady Biochem. Biophys.* **2007**, *415*, 211.
[25] N. Terasaki, M. Iwai, N. Yamamoto, T. Hiraga, S. Yamada, Y. Inoue, *Thin Solid Films* **2008**, *516*, 2553.
[26] S. C. Tan, L. I. Crouch, M. R. Jones, M. Welland, *Angew. Chem. Int. Ed.* **2012**, *51*, 6667.
[27] A. W. Roszak, T. D. Howard, J. Southall, A. T. Gardiner, C. J. Law, N. W. Isaacs, R. J. Cogdell, *Science* **2003**, *302*, 1969.
[28] S. C. Tan, L. I. Crouch, S. Mahajan, M. R. Jones, M. E. Welland, *ACS Nano* **2012**, *6*, 9103.
[29] C. Zhang, F. Yan, C. S. Allen, B. C. Bayer, S. Hofmann, B. J. Hickey, D. Cott, G. Zhong, J. Robertson, *J. Appl. Phys.* **2010**, *108*, 024311.
[30] Y. Tsuji, Y. Tsuji, S. Nakamura, S. Noda, *Appl. Surf. Sci.* **2010**, *256*, 7118.
[31] S. C. Tan, L. Liu, Y. P. Zeng, A. See, Z. X. Shen, *J. Electrochem. Soc.* **2005**, *152*, G754.
[32] K. K. S. Lau, J Bico, K. B. K. Teo, M. Chhowalla, G. A. J. Amaratunga, W. I. Milne, G. H. Mckinley, K. K. Gleeson, *Nano Lett.* **2003**, *3*, 1701.

[33] C. T. Wirth, S. Hofmann, J. Robertson, *Diamond Relat. Mater.* **2008**, *17*, 1518.
[34] S. Esconjauregui, B. C. Bayer, M. Fouquet, C. T. Wirth, C. Ducati, S. Hofmann, J. Robertson, *Appl. Phys. Lett.* **2009**, *95*, 173115.
[35] Q. W. Jiang, G. R. Li, X. P. Gao, *Chem. Commun.* **2009**, *22*, 6720.
[36] E. M. Gullikson, A. P. Mills, J. M. Phillips, *Surf. Sci.* **1988**, *195*, L150.
[37] C. Pirri, J. C. Peruchetti, G. Gewinner, J. Derrien, *Surf. Sci.* **1985**, *152*, 1106.
[38] J. Westlinder, T. Schram, L. Pantisano, E. Cartier, A. Kerber, G. S. Lujan, J. Olsson, G. Groeseneken, *IEEE Electron Device Lett.* **2003**, *24*, 550.
[39] M. Shiraishi, M. Ata, *Carbon* **2001**, *39*, 1913.
[40] V. S. F. Chew, J. R. Bolton, *J. Phys. Chem.* **1980**, *84*, 1903.
[41] F. Kreupl, A. P. Graham, G. S. Duesberg, W. Steinhogl, M. Liebau, E. Unger, W. Honlein, *Microelectron. Eng.* **2002**, *64*, 399.
[42] C. O'Regan, A. Lee, J. D. Holmes, N. Petkov, P. Trompenaars, H. Mulders, *J. Vac. Sci. Technol. B* **2013**, *31*, 021807.
[43] N. Arshi, J. Lu, Y. K. Joo, C. G. Lee, J. H. Yoon, F. Ahmed, *J. Mater. Sci.: Mater. Electron.* **2013**, *24*, 1194.
[44] N. P. Reynolds, S. Janusz, M. Escalante-Marun, J. Timney, R. E. Ducker, J. D. Olsen, C. Otto, V. Subramaniam, G. J. Leggett, C. N. Hunter, *J. Am. Chem. Soc.* **2007**, *129*, 14625.
[45] M. F. Richter, J. Baier, T. Prem, S. Oellerich, F. Francia, G. Venturoli, D. Oesterhelt, J. Southall, R. J. Cogdell, J. Kohler, *Proc. Natl. Acad. Sci. USA* **2007**, *104*, 6661.
[46] M. Kondo, K. Iida, T. Dewa, H. Tanaka, T. Ogawa, S. Nagashima, K. V. P. Nagashima, K. Shimada, H. Hashimoto, A. T. Gardiner, R. J. Cogdell, M. Nango, *Biomacromolecules* **2012**, *13*, 432.
[47] D. Gerster, J. Reichert, H. Bi, J. V. Barth, S. M. Kaniber, A. W. Holleitner, I. Visoly-Fisher, S. Sergani, I. Carmeli, *Nat. Nanotechnol.* **2012**, *7*, 673.